Research Paper

PAIN®

OPEN

The effect of early procedural pain in preterm infants on the maturation of electroencephalogram and heart rate variability

Mario Lavanga[a,*], Bieke Bollen[b], Alexander Caicedo[c], Anneleen Dereymaeker[b], Katrien Jansen[b], Els Ortibus[b], Sabine Van Huffel[a], Gunnar Naulaers[b]

Abstract

Preterm infants show a higher incidence of cognitive, social, and behavioral problems, even in the absence of major medical complications during their stay in the neonatal intensive care unit (NICU). Several authors suggest that early-life experience of stress and procedural pain could impact cerebral development and maturation resulting in an altered development of cognition, behavior, or motor patterns in later life. However, it remains very difficult to assess this impact of procedural pain on physiological development. This study describes the maturation of electroencephalogram (EEG) signals and heart rate variability in a prospective cohort of 92 preterm infants (<34 weeks gestational age) during their NICU stay. We took into account the number of noxious, ie, skin-breaking, procedures they were subjected in the first 5 days of life, which corresponded to a median age of 31 weeks and 4 days. Using physiological signal modelling, this study shows that a high exposure to early procedural pain, measured as skin-breaking procedures, increased the level of discontinuity in both EEG and heart rate variability in preterm infants. These findings have also been confirmed in a subset of the most vulnerable preterm infants with a gestational age lower than 29 weeks. We conclude that a high level of early pain exposure in the NICU increases the level of functional dysmaturity, which can ultimately impact preterm infants' future developmental outcome.

Keywords: Pain, Stress, Skin-breaking procedure, EEG, HRV, Development, Premature infants

1. Introduction

The survival rates of preterm infants increased in recent years, but the incidence of cognitive and behavioral deficits remains higher than in full-term infants even in the absence of specific cerebral lesions.[34] Different authors describe that between 30% and 60% of the preterm population show a lower cognitive and/or behavioral outcome compared to their peers,[33,35] without necessarily showing any specific complication during their stay in the neonatal intensive care unit (NICU).[5]

Several authors suggest that pain-related stress and repeated procedural pain could play a role in the altered development of cognition, behavior, and motor patterns of premature infants.[21,48,53] Early-life painful experiences seem to impact the brain structure and function on the cortical and subcortical levels.[17,45,48] Both frontal and parietal cortex volumes and thickness have been found to decrease in case of procedural pain.[45,48] Similarly, white matter connectivity and thalamic volume are reduced in case of high numbers of early skin-breaking procedures (SBPs), which count events like heel lance, intramuscular injection, chest tube insertion, and central line insertion.[8,17] Therefore, the accumulation of procedural pain in the NICU might play a role in the lower cognitive and behavioral outcome. For example, Grunau et al[22] found lower cognitive outcome scores at 18 months and more internalizing behavior in preterm infants that underwent a high number of SBPs.

The impact of early-life pain on brain development can be assessed through magnetic resonance imaging (MRI). This technique, which mainly shows anatomical abnormalities, is not always available for preterm babies.[36] Electroencephalogram (EEG) is a complementary technique, which provides insights in functional brain integrity and has the advantage of being less invasive. The sensitization to pain and the lowering pain threshold in premature infants[19,22] can affect the subplate neurons through excitotoxicity and apoptosis,[53] resulting in changes in brain volumes. Pain sensitization, intended as capacity to discriminate noxious stimuli, can be measured in preterm infants by means of cortical reactivity responses to the heel lance.[18,19] Those evoked potentials normally are dispersed neuronal bursts on the scalp up to 35-week gestational age (GA)[18,47] and they are replaced by mature evoked responses contributing to the EEG background progression from a discontinuous to a continuous trace.[42] Therefore, one might also expect alterations of the spontaneous background cortical oscillations due to pain-related stress.[16] In addition, Jones et al[26] highlighted the relationship between infants' heart rate variability (HRV) and EEG evoked-potentials to noxious stimuli, whereas Cong

Sponsorships or competing interests that may be relevant to content are disclosed at the end of this article.

[a] Department of Electrical Engineering (ESAT), Division STADIUS, KU Leuven, Leuven, Belgium, [b] Department of Development and Regeneration, Faculty of Medicine, KU Leuven, Leuven, Belgium, [c] Department of Applied Mathematics and Computer Science, School of Engineering, Science and Technology, Universidad Del Rosario, Bogota', Colombia

**Corresponding author. Address: Department of Electrical Engineering (ESAT), Division STADIUS, KU Leuven, Kasteelpark Arenberg 10, bus 2446, 3001, Leuven, Belgium. Tel.: +33 6 52 93 31 80. E-mail address: mlavanga@esat.kuleuven.be (M. Lavanga).*

PAIN 162 (2021) 1556–1566

http://dx.doi.org/10.1097/j.pain.0000000000002125

et al[10] showed specific changes in HRV in response to heel lance in premature infants.

We hypothesized that pain-related stress increases electrophysiological dysmaturity, ie, a higher EEG discontinuity due to a higher number of dispersed neuronal bursts and a higher HRV of long-term oscillations. A quantitative analysis of EEG and HRV was used to monitor decreasing rate of EEG discontinuity and increasing HRV, respectively.[23,31,32,41,55] Specifically, functional maturation charts were obtained to understand whether a high level of SBPs can induce dysmature patterns in EEG and HRV, suggesting an impact on the developmental outcome of the patient.

2. Methods

The research protocol was examined and approved by the Ethical Committee of University Hospitals Leuven (Belgium) as part of the Resilience trial, which was registered at Clinical Trials.gov (NCT02623400). The study was performed in accordance with the Guidelines for Good Clinical Practice (ICH/GCP) and the latest version of the Declaration of Helsinki.

2.1. Participants

A prospective cohort of (n = 92) preterm infants was recruited in the NICU of the University Hospitals Leuven (Belgium) between July 2016 and July 2018, as part of a larger ongoing study on preterm infant and parental resilience.

Parents of preterm infants born before 34-week GA and/or with a birth weight (BW) less than 1500 g were approached for informed consent within the first 3 days after birth. Exclusion criteria were parental age <18 years, medical (somatic or psychiatric) condition in parent(s) that impeded participation, absence or limited knowledge of Dutch or English, major congenital malformation, or central nervous system pathology (grade 3 or grade 4 intraventricular hemorrhage or periventricular leukomalacia—brain ultrasounds were conducted on postnatal days 1, 3, and 7, and then repeated weekly) in the preterm infant at the time of consent.

2.2. Data acquisition

Medical and nursing electronic charts were reviewed from birth till discharge home by a physician and by 2 GCP-qualified neonatal research nurses. Variables that were obtained included GA at birth, BW, illness severity at birth (eg, clinical risk index for babies - CRIB score[49]), and the number of SBPs per day. Also, data on neuroactive medications (caffeine, dopram, fentanyl, luminal, chloral hydrate, dormicum, contramal, and catapressan) administered on the day of the recording were obtained. Caffeine was routinely administered at a dose of 5 mg/kg.

Neonatal procedural pain exposure was defined as the sum of all SBPs. To define these SBPs, we drew on the work of Brummelte et al[8] and Grunau et al,[22] as well as the work of Newnham et al. (2009) in the development of the Neonatal Infants Stress Scale (NISS). We included medical procedures that yield a score of 4 and 5 on the NISS such as chest tube insertion, central line insertion, heel lance, intramuscular injection, eye examination, and other added nursing procedures such as wound care. An overview of all procedures is reported in **Table 1**. Skin-breaking procedures were counted for every category separately for each day. If multiple attempts were conducted, each attempt was counted as a single SBP.

We calculated the sum of SBPs in the first 5 days of life. Subsequently, SBP scores were binarized (LOW SBPs vs HIGH SBPs) with a threshold of 50 SBPs in the first 5 days of life to detect patients who experienced a high number of SBPs, and thus a high level of early procedural pain. This threshold was based on earlier findings on the impact of early-life SBPs in preterm infants[8,17] and our analysis of the distribution of the cumulative SBPs (discussed in the results section). This makes it possible to compare the neuroanatomical changes reported by these authors with the neurophysiological changes that we describe. Brummelte et al[8] and Duerden et al[17] considered procedural pain as the cumulated SBP up to their first MRI scan (normally around postmenstrual age [PMA] 32 weeks or 21 postnatal days). Our first recording was planned to be as close as possible to postnatal day 5. However, sometimes it had to be conducted a few days earlier or later because of the preterm infant's unstable medical condition, or because of EEG equipment or technician availability.

2.3. Electrophysiological data collection

Physiological data were measured at 3 different time points in each patient. The recording protocol comprised a first measurement within 5 days from birth (5 days), another session at 34 weeks PMA (34w), and a last measurement before discharge to home. Measurements lasted for at least 3 hours as a rule, infants underwent a 24-hour polysomnography (PSG) before leaving the NICU, and therefore the last session was labeled as PSG. For some patients, the recording schedule was adapted. For infants born at 33 to 34 weeks GA, only one recording (representing the first 2 coinciding recordings from birth) was performed because their PMA was around 34w when they were 5 days old. Some infants were transferred to level II units in hospitals closer to home. Therefore, not all infants have multiple recordings and, importantly, some SBP measures could not be tracked. However, we strived for the readmission of infants to our hospital for the PSG measurement before they went home. In total, 92 patients with 228 recordings and information about the number of SBPs were analyzed. The Gantt chart in **Figure 1** summarizes the number of recordings and cumulated SBPs at the different timestamps. More details are reported in the statistical analysis section.

Physiological data included EEG and ECG measurements. EEG data were collected according to the 10 to 20 system using 9 monopolar electrodes (Fp1, Fp2, C_3, C_4, C_z, T_3, T_4, O_1, O_2) and monitored with the OSG system (OSG BVBA, Brussels). Each EEG signal was referenced to C_z, which was then excluded from further analysis, leaving a total amount of 8 channels. ECG was measured as single lead ECG and was used to derive the tachogram or HRV signal as subsequent R-peak to R-peak intervals. The R-DECO toolbox[37] was used for R-peak detection.

Before any functional analysis, both EEG and HRV signals were preprocessed to remove artefacts and define sleep states. To remove movement-related and noncortical information, EEG signals were band-pass-filtered between 0.5 and 20 Hz and independent component analysis to filter electrooculogram was then applied. The narrow filtering band is based on the quantitative analysis of discontinuous EEGs by De Wel et al[55] and of amplitude-integrated EEGs by O'Toole et al.[40]

EEG data were then used to define 2 processing epochs of 20 minutes each related to quiet sleep state and a combination of awake and active sleep, which is called *nonQuiet sleep* (nQS). The behavioral analysis was performed with the algorithms described in,[2,14] the probabilistic output of which was summed to look for the two 20-minute epochs. Quiet sleep (QS) was derived as a window around the maximum of a quiet-sleep probability profile, whereas nQS as a window around the minimum.

Table 1

Overview of all different SBP categories monitored in the study.

SBP categories: Punctures	SBP categories: Ventilation	SBP categories: Other
Venous or arterial blood sample	Placing CPAP tube	Placing thorax drain
Placing peripheral venous catheter	Endotracheal aspiration	Care thorax drain
Placing deep venous catheter	Aspiration mouth and nose	Placement gastrointestinal tube
Placing umbilical arterial and/or venous catheter		Wound care
Lumbar punction		Surgery
Intubation		Eye examination

The first column is related to all puncture procedures, the second column is related to ventilation procedures, and the last one is related to other painful procedures.
CPAP, continuous positive airway pressure; SBP, skin-breaking procedures.

Before the extraction of any functional feature, the last step of the preprocessing for both sleep stage epochs was a segmentation in nonoverlapping sliding windows and a threshold filtering according to the following criteria: SD above 50 μV, absolute difference sample-to-sample above 50 μV, and absolute amplitude above 200 μV.[24] The size of each window was different for each extracted variable and is specified in following subparagraphs. It is important to highlight that a window was excluded from the processing if more than 4 channels exceeded one of the criteria thresholds.

Because the RR intervals of the tachogram can be affected by premature ventricular contractions (PVC), the RR were corrected [37] and the modulation signal m(t) was derived using the *integral pulse frequency modulation* model to investigate the autonomic nervous system stimulation.[3]

2.4. Functional measurements

Different features were computed to track the functional maturation of neonates during their NICU stay and assess the level of dysmaturity in the electrophysiological signals, based on previous studies.[23,41,55] Dysmaturity in EEG signals was defined as a discontinuity and persistence of delta waves,[51] whereas dysmaturity of HRV was defined as a higher amplitude of the slow-wave oscillations.[25] The computational steps to derive EEG and HRV dysmature patterns are reported in the paragraph below.

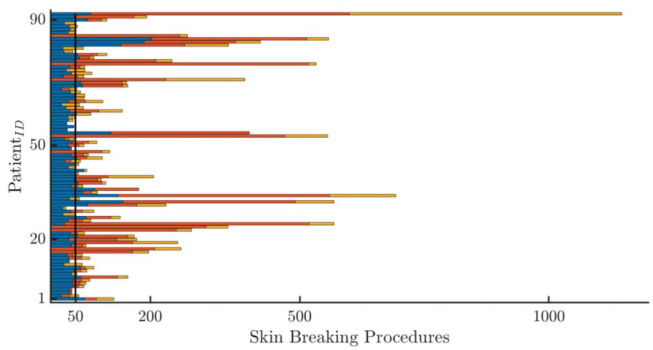

Figure 1. An overview of all recordings in the data set. The Gantt-chart-like overview of all recordings for the different patients. The number of stacked bars represents the number of recordings and the color is associated for the recording time: blue for the first recording, red for the second recording at 34 w, and the yellow is the recording at discharge (PSG). The length represents the cumulative amount of SBPs. In particular, the blue bar is the cumulated SBPs up to first recording, whereas the red and the yellow bars have the incremental values of cumulated SBPs with respect to the first recording. SBP, skin-breaking procedures.

2.4.1. Amplitude-integrated EEG features

Clinicians normally rely on the amplitude-integrated EEG (aEEG) for the assessment of brain maturity and the emergence of sleep-wake cycle. The great advantage is the simplicity of interpretation compared to a full-channel EEG.[43] Therefore, we decided to quantify the level of EEG dysmaturity with a more interpretable metric. The aEEG was estimated by means of the range EEG and the discontinuity of EEG features was quantified by means of range EEG (rEEG) asymmetry.[41] This variable quantifies the level of dysmaturity by the difference in distance from the rEEG median to lower and upper margin of rEEG itself. These 2 margins represent, respectively, the 5th and 95th percentiles of the rEEG.[38] Studies show the higher the asymmetry, the higher the discontinuity of EEG.[39,41] Following the guidelines,[41] the asymmetry was derived for the most important EEG frequency bands, which are $\delta = (2-4)$ Hz, $\theta = (4-8)$ Hz, $\alpha = (8-16)$ Hz, and $\beta = (16-20)$ Hz. The rEEG is computed for each channel and one signal is obtained by the median of all range EEGs to resemble the approach of aEEG. The rEEG was derived for 2-second windows without overlap and all indices were then grand-averaged for each sleep state.

2.4.2. Multiscale entropy

A more refined maturity index of the neonatal EEG is the multiscale entropy (MSE).[7,11,55] It is based on the more common index of the Sample Entropy, which measures the predictability of the signal. Its actual definition is the negative natural logarithm of the conditional probability that a data set of size N, which presents repetition of an m-points pattern with a certain tolerance r, will also present repetition of an $m+1$ points pattern within the same tolerance.[30] The tolerance r is normally defined as 20% of the SD of the signal. The MSE is a generalized version of Sample Entropy at different scales τ, which means the signal is coarsely grained with a moving average and downsample of order τ. The advantage is 2-fold: MSE does not only contain the information of the regular Sample Entropy at scale 1, but the coarse-graining process enhances the slower patterns in the computation of the sample entropy.

In general, the Sample Entropy is low in case of discontinuity and early-life EEG and increases with age.[56] Similarly, the area under the MSE curve or the cumulated MSE for all scales, $\mathrm{CI} = \sum_{\tau} \mathrm{MSE}\ (\tau)$, is low in case of discontinuity and it increases with age.[55] This metric is known as the complexity index (CI) and is a general measure of irregularity across scales. Therefore, the MSE will investigate how the matching probability varies for long-term variations (high scales or low frequencies) and for short-term variations (small scales or high frequencies), combining both the investigation of EEG discontinuity and slow-wave patterns.

Complexity index was computed in 150-second nonoverlapping windows and grand-averaged along the time course of each sleep

Table 2

Summary of patient data set at different time points: SBPs (skin-breaking procedure at 5 days), GA (gestational age in weeks), birth weight (in g), PMA (postmenstrual age in weeks) at different recording dates (5 days, 34w, PSG), CRIB score, APGAR score at 5 minutes from birth, and the number of days in mechanical ventilation and continuous positive airway pressure, caffeine treatment (number of patients receiving treatment, standard dose 5 mg/kg) at first and second EEG measurements, and the ultrasound evaluation.

	HIGH SBP (n = 19)	LOW SBPs (n = 73)	*P*
SBPs	60 [56.25-69.5]	31 [24-37]	≤0.01
GA (weeks)	26.57 [25.29-29.5]	32 [29.5-32.57]	≤0.01
PMA at 5 days (first rec)	28.57 [26.43-31.57]	32.86 [31-33.57]	≤0.01
PMA at 34w (second rec)	34.29 [33.71-34.29]	34.07 [33.86-34.29]	0.32
PMA at PSG (third rec)	39.93 [38.71-42]	38.43 [37.36-39.21]	≤0.01
Birth weight (g)	950 [820-1137.5]	1540 [1230-1800]	≤0.01
CRIB score	2 [1-4.75]	0 [0-1]	≤0.01
APGAR 5 min	8 [6.25-9]	8 [6-8]	0.14
Days of mechanical ventilation	2.5 [0-16.5]	0 [0-0]	≤0.01
Days of CPAP	41.5 [7.75-55.5]	4 [2-28]	≤0.01
Caffeine (at 5 days)	17	63	0.715
Caffeine (at 34w)	15	31	≤0.05

Data are split in HIGH SBP (SBP ≥50) and LOW SBP (SBP <50). Data are median [IQR] except for the caffeine treatment. Data were compared between the low and high SBP groups using Mann–Whitney *U*tests for continuous variables and χ^2 tests for categorical variables.
SBP, skin-breaking procedures; PMA, postmenstrual age.

state.[15,44,55] Multiscale entropy was computed for each channel, and each of these complexity indices was considered in the final procedural pain analysis.

2.4.3. Heart rate variability power features

To assess dysmaturity based on the autonomic activity, the absolute power of the HRV in the high-frequency (HF), low-frequency (LF), and very-low frequency (VLF) bands was computed. The band limits were the following ones: HF = (0.2 − 4) Hz, LF = (0.08 − 0.2) Hz, and VLF = (0.0033 − 0.08) Hz.[13] The power spectral density was computed using the continuous wavelet transform (CWT), with analytical Morlet as mother wavelet. The CWT computes an instantaneous power spectrum of the signal and the band-power can then be computed for each time sample. Consequently, power time-series are obtained for the LF, HF, and VLF power. The CWT was estimated in both QS and nQS using the entire 20 minutes and power time-series were averaged over both epochs.

2.5. Statistical analysis

Statistical analysis was performed with MatLab (Mathworks, Inc). A linear mixed-effect regression (LME) model was performed to evaluate the association between functional measurements (HRV

Table 3

Summary of most vulnerable patient data with GA ≤29 weeks: SBP (skin-breaking procedure at 5 days), GA (gestational age in weeks), birth weight (in g), PMA (postmenstrual age in weeks) at different recording dates (5 days, 34w, PSG), CRIB score, APGAR at 5 minutes from birth, the number of days in mechanical ventilation and continuous positive airway pressure, caffeine treatment (number of patients receiving treatment, standard dose 5 mg/kg) at first and second EEG measurements and the ultrasound evaluation.

	HIGH SBP (n = 14)	LOW SBP (n = 17)	*P*
SBP	65.5 [58-73]	40 [32-44]	≤0.01
GA	26.14 [25.14-26.86]	28.43 [26.71-28.71]	≤0.01
PMA at 5 days (First rec)	26.57 [26.21-28.64]	29.43 [27.54-29.68]	0.05
PMA at 34w (Second rec)	34.29 [34-34.29]	34 [33.86-34.14]	0.08
PMA at PSG (Third rec)	39.93 [39.29-42]	38.64 [38.14-40]	0.08
Birth weight	890 [800-1050]	1090 [905.5-1203.25]	0.1
CRIB score	2.5 [1-6]	2 [1-4.5]	0.64
APGAR 5 min	8 [5.75-9]	8 [6-8.75]	0.95
Days of mechanical ventilation	9 [0-19]	1 [0-1.5]	0.20
Days of CPAP	44 [35-80.5]	44 [36-55]	0.71
Caffeine (at 5 days)	12	14	0.80
Caffeine (at 34w)	12	16	0.43

Data are split in HIGH SBP (SBP ≥50) and LOW SBP (SBP <50). Data are median [IQR] except for the caffeine treatment. Data were compared between the low and high SBP groups using Mann–Whitney *U*tests for continuous variables and χ^2 tests for categorical variables.
SBP, skin-breaking procedures.

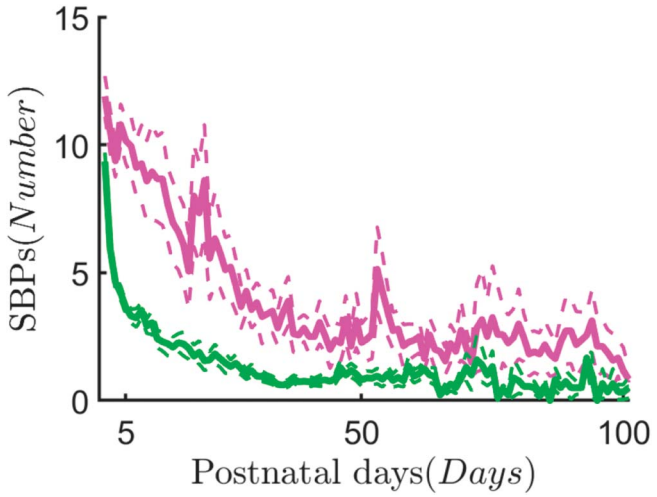

Figure 2. The average skin-breaking procedures during the NICU stay. The chart of the skin-breaking procedures is displayed as average over the different patients in the 2 groups, HIGH SBPs (SBPs ≥ 50) in magenta and LOW SBPs (SBPs < 50) in green. The curves show the SBP dynamics during the neonatal intensive care unit stay in the first 100 days. The average chart is represented by the continuous thick line, whereas the upper bound and the lower bound represent the error margin. The curve has been defined as $\mu(t) \pm \frac{\sigma(t)}{\sqrt{N(t)}}$, where $\mu(t)$ is the mean of the patient distribution, $\sigma(t)$ is the SD, and N(t) represents the number of patients. The variable t represents each postnatal day. The exponential decay highlights that most procedural pain is concentrated in the first days of life. NICU, neonatal intensive care unit; SBP, skin-breaking procedures.

power, EEG complexity, and asymmetry) and early SBPs. To correct for the effect of GA and PMA, the final regression model did not only include the binary SBP, but also these 2 age-related variables as fixed effects. The random effect was expressed by the group represented by each patient and was considered for both the slope coefficients and the intercept of the LME model. In addition, the regression models were computed for both behavorial sleep states (QS and nQS).

The significance of the association between early SBPs and functional measurements was tested in 2 ways. To correct for the multiple comparisons (multiple features coming from multiple channels), the *P*-value of the SBP coefficient was corrected using the false-discovery rate with $\alpha = 0.05$. The false-discovery rate (FDR) can be applied to correct for the number of brain region locations in case of channel-dependent features,[17,45] but it can also be used to correct for the total number of extracted features.[20,27] False-discovery rate was applied in our study to correct for the number of features in the analysis and rank the features from the one with most significant association with SBPs to the least significant one. In addition, the significant contribution of SBP in explaining the maturational trajectory of the functional variables was assessed using the log-likelihood ratio (LLR) test.[4] This ratio test specifically assesses whether adding "early SBPs" in the prediction model reduces the variance of the residuals of a model, which contains only the age variables (PMA and GA). The full coefficient of determination (R^2) of the model including SBP group as well as the coefficient of determination of the reduced model, with only GA and PMA (R^2_{Red}), was also computed. The decrease in error (%) when the SBP variable is added to the model was also obtained together with the associated log-likelihood statistics F, which is ultimately a log transform of the error variances ratio.

In addition, two-way analyses of variance (ANOVAs) were performed on our EEG and HRV variables of interest with SBP group (low vs high) and measuring point (5 days, 34 weeks, PSG) as independent variables. To investigate differences between preterm infants in the high and low SBP at each measuring point, Tukey–Kramer multiple comparison tests were subsequently performed.

These models were tested for both the entire set of patients (n = 92) and for preterm infants with a GA ≤29 weeks (n = 31). We specifically focus on this more coherent group of extremely preterm babies because they are most vulnerable to require intensive care and are thus subjected to more SBPs.

3. Results

3.1. Patients demographics

Infant demographics and clinical characteristics are summarized in **Table 2** for the entire data set and in **Table 3** for the early-GA data set. As expected, patients with a higher number of cumulated SBPs at 5 days also had a lower GA, a lower PMA at the moment of the recording, higher CRIB score, and higher number of days of mechanical ventilation and of continuous positive airway pressure (**Table 2**). Caffeine treatment (yes/no) at 5 days and APGAR score did not significantly differ between SBP groups, whereas the number of patients receiving caffeine was different at 34 weeks between SPB groups. In the subset of early-GA infants (<29 weeks), only BW differed significantly between infants of the low and high SBP groups (**Table 3**). Only one patient from the high SBP group received medication that could exert a central nervous system depressant effect at the 34-week recording. However, the patient was kept in the overall analysis because the medication was only provided during one recording of the patient and because we did not observe

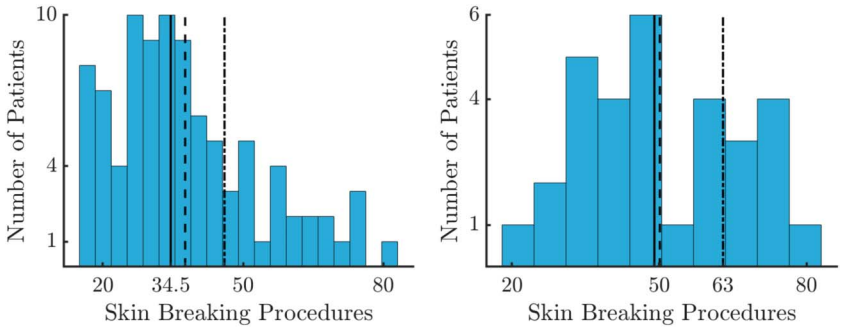

Figure 3. Distributions of SBPs data at 5 days. The histogram distributions for the cumulative amount of SBPs at 5 days from birth. The right panel shows the distribution for the entire data set, whereas the second one depicts the distribution for the low gestational age data set (GA ≤ 29 weeks). The black continuous line represents the median value of the distribution, the dashed line represents the mean, and the dotted dashed line is 75% quantile of the investigated distribution. GA, gestational age; SBP, skin-breaking procedures.

Table 4

Results of the linear mixed effect model for the nonquiet sleep (nQS) state in the ENTIRE data set.

Feature	B_{SBP}	B_{GA}	B_{PMA}	MSE	R^2	R^2_{Red}	F_{LLR}	Δ(%)
CI(Fp2)	−1.585‡	0.241‡	0.669*	8.04	0.48	0.46	6.93‡	3.23
P(HF)	0.003‡	0.00008§	0.00046*	0.00002	0.21	0.09	9.7†	4.49
CI(T4)	−1.333‡	0.266†	0.541*	7.11	0.42	0.4	6.58‡	3.07
CI(O2)	−1.229‡	0.214‡	0.691*	6.578	0.53	0.51	6.84‡	3.19

Only the features that have a significant association with early skin-breaking procedure are reported. The values B represent the fixed-effect coefficients for the SBP, GA, and PMA variables with the associated significance level (*P* value). For each feature, the following parameters are reported: the mean-absolute error (MSE), the coefficient of determination R^2, the coefficient of determination of the model with only GA and PMA (R^2_{Red}), the log-likelihood ratio (LLR) F-statistics, and the decrease of error variance Δ(%) with SBPs variable. The *P* value is indicated with following symbols: * for *P* value ≤ 0.0001, † for *P* ≤ 0.01, ‡ for *P* ≤ 0.05, and § for not significant *P* values. CI stands for complexity index and P(HF) stands for HF power in the tachogram.

SBP, skin-breaking procedures; PMA, postmenstrual age.

significant changes in the regression models when this recording was omitted.

3.2. Skin-breaking procedures

Figure 2 clearly shows that there is a peak in the number of SBPs in the first days of life, followed by an exponential decay. In particular, there is already a significant drop in SBPs after 5 postnatal days. The distribution of cumulated SBPs at 5 days is reported for the entire data set and for the subset of patients with GA ≤29 weeks in **Figure 3**. In the entire data set, the median number of cumulated SBPs at 5 days is 34.5 and the distribution has a fat-tail on the right. It implies that a median threshold would give rise to more heterogeneous levels of SBPs in the high SBP group. The early-GA distribution has a median of 50 without a fat-tail; therefore, it contains more similar high-level SBPs. Importantly, **Figure 2** shows that, using this threshold, the difference in the number of SBPs persists throughout NICU stay between preterm infants in the low and high SBP groups.

3.3. Relationship between EEG and heart rate variability functional variables and early skin-breaking procedures

The relationship between electrophysiological maturational trends and early SBPs was examined for the entire data set and reported in **Tables 4 and 5**. After FDR correction, early SBPs were negatively associated with the EEG CI, during QS as well as nQS (eg, CI(FP2) has $B_{SBP} = -1.585$ with $P \leq 0.05$ in nQS and CI(C3) has $B_{SBP} = -2.23$ with $P \leq 0.05$ in QS). Early SBPs were also associated to an increase in range EEG asymmetry in QS (eg, asym(θ) with $B_{SBP} = 0.051$ with $P \leq 0.01$). For HRV, the power in the HF band was positively associated with SBPs in both QS and nQS (P(HF) has $B_{SBP} = 0.003$ with $P \leq 0.05$ and has $B_{SBP} = 0.003$ with $P \leq 0.01$ in QS). These results imply that a high level of SBPs is associated with a discontinuous EEG trace and with a higher vagal tone after PMA and GA correction.

The central role of SBPs is confirmed by the LLR test and the decrease in error variance reported in **Tables 4 and 5**. In nQS, the decrease in error variance ranges from 3.07% to 4.49% with an associated improvement of R^2 from R^2_{Red}, whereas the decrease oscillates between 2.95% up to 10% in the QS epoch. All the reported variables had significant improvement in the regression performance as indicated by the associated *P*-values.

The differences in maturational trends reported by **Tables 4 and 5** are investigated at each recording time using the 2-way ANOVA test. Based on the FDR ranking in **Tables 4 and 5**, we reported CI(FP2) in nQS, asym(θ) in QS and P(HF) in QS in **Figures 4–6**.

In nonquiet sleep, we found a statistically significant interaction effect between measuring point and SBP group on EEG CI

Table 5

Results of the linear mixed-effect model for the QUIET sleep (QS) state in the ENTIRE data set.

Feature	B_{SBP}	B_{GA}	B_{PMA}	MSE	R^2	R^2_{Red}	F_{LLR}	Δ(%)
Asym(θ)	0.051†	0.002§	−0.023*	0.005	0.62	0.56	12.72†	5.85
CI(C3)	−2.223†	−0.182§	1.077*	9.739	0.62	0.59	11.68†	5.39
P(HF)	0.003†	0.00015§	0.0003†	0.00002	0.13	0.01	22.41†	10.1
Asym(δ)	0.048†	0.004§	−0.021*	0.005	0.55	0.491	1.02†	5.09
Asym(α)	0.056†	0.006‡	−0.022*	0.006	0.56	0.45	9.65†	4.47
CI(Fp2)	−1.759†	−0.211‡	1.05*	7.93	0.65	0.63	8.78‡	4.08
CI(O1)	−2.137†	−0.176§	1.041*	8.828	0.63	0.59	10.53†	4.87
CI(O2)	−1.705‡	−0.143§	1.031*	7.468	0.67	0.61	9.03‡	4.19
CI(Fp1)	−1.628‡	−0.256‡	1.058*	8.096	0.65	0.63	7.03‡	3.28
CI(T3)	−1.771‡	−0.099§	1.027*	6.186	0.73	0.64	9.23‡	4.28
Asym(β)	0.047‡	0.005§	−0.02*	0.005	0.53	0.41	7.29‡	3.4
CI(T4)	−1.626‡	−0.133§	1.017*	6.83	0.72	0.6	6.33‡	2.95

Only the features that have a significant association with early skin-breaking procedure are reported. The values B represent the fixed-effect coefficients for the SBP, GA, and PMA variables with the associated significance level (*P* value). For each feature, the following parameters are reported: the mean-absolute error (MSE), the coefficient of determination R^2, the coefficient of determination of the model with only GA and PMA (R^2_{Red}), the log-likelihood ratio (LLR) F-statistics, the decrease of error variance Δ(%) with SBPs variable, and the two-way ANOVA *P* value associated with the SBP main effect. The *P* value is indicated with following symbols: * for *P* value ≤ 0.0001, † for *P* ≤ 0.01, ‡for *P* ≤ 0.05, and § for not significant *P* values. CI stands for complexity index, P(HF) stands for HF power in the tachogram, and asymmetry is the asymmetry of rEEG in the different frequency bands.

ANOVA, analysis of variance; SBP, skin-breaking procedures.

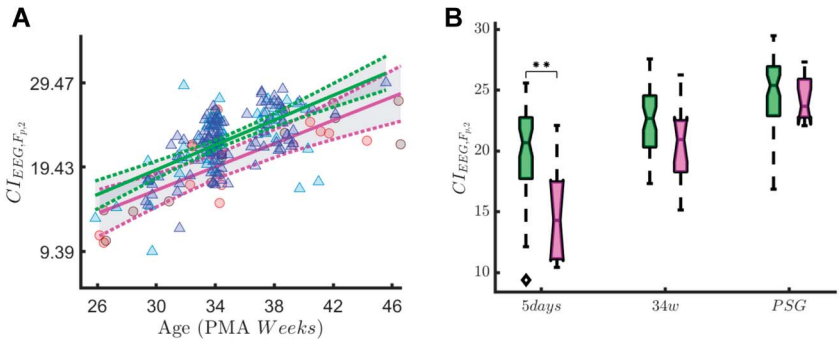

Figure 4. Complexity index (CI) in nonquiet sleep. The figure shows the association with CI and early skin-breaking procedure (SBPs). Data are reported for the entire data set during nQS. The left panel shows how the CI maturational trend differs in case of high SBPs (magenta curve, SBPs ≥50) compared to low SBPs (green curve, SBP <50). The blue/green triangles represent the patient with low SBPs (N = 73) and red/orange circles the high SBPs (N = 19). The right panel shows the boxplot trend as output of the two-way ANOVA: the division between HIGH SBPs and LOW SBPs is reported for each recording time. The CI increases over time (main effect of measuring point: F(2,178) = 42.17, $P \leq 0.01$), but statistically significant interaction effect between measuring point and SBPs group is found (F(2,178) = 6.62, $P \leq 0.01$). The simple main-effect analysis shows a lower complexity in HIGH SBPs group at the 5-day recording ($P \leq 0.01$, indicated as ** in the figure), but there is no significant difference for the 34-week ($P = 0.59$) or PSG ($P = 1$) recording time. ANOVA, analysis of variance.

(F(2,178) = 6.62, $P \leq 0.01$). **Figure 4** shows that the CI increases over time (main effect of measuring point: F(2,178) = 42.17, $P \leq 0.01$). Simple main-effects analysis showed that preterm infants in the high SBP group have a lower CI than children in the low SBP group at the 5-day recording ($P \leq 0.01$). This difference is not statistically significant for the 34 weeks ($P = 0.59$) or PSG ($P = 1$) recording.

In quiet sleep, we found a statistically significant measuring point-by-SBPs group interaction effect for asym(θ) (F(2,208) = 8.52, $P \leq 0.01$, **Figure 5**). As expected, rEEG asymmetry decreased over time (main effect of measuring point F(2,208) = 101.71, $P \leq 0.01$). Simple main-effects analysis showed a higher rEEG asymmetry in preterm infants in the high SBP group compared to the low SBP group at the first measuring point at 5 days ($P \leq 0.01$). This difference was still marginally significant at the 34-week recording ($P = 0.05$). For the last recording (PSG), rEEG asymmetry did not statistically differ between the low and high SBPs groups ($P = 0.72$). **Figure 6** shows that the HF oscillations increase over time (main effect of measuring point: F(2,191) = 5.97, $P \leq 0.01$), but statistically significant interaction effect between measuring point and SBP group is found (F(2,191) = 4.56, $P \leq 0.01$). The simple main-effect analysis shows a higher P(HF) in the high SBPs group at the PSG recording time ($P \leq 0.01$), but there is no difference for the 5-day ($P = 0.43$) or 34w ($P = 1$) recording time.

The results for the patients with a GA below 29 weeks are reported in **Table 6** only for QS. The variables in nQS did not pass the FDR test. Similarly to the entire data set, the HF power and the asymmetry in the alpha and theta bands in QS have a positive association with the SBPs variable (P(HF) has $B_{SBP} = 0.005$ with $P < 0.01$ and asym(alpha) has $B_{SBP} = 0.064$ with $P \leq 0.05$). Unlike the entire data set, the sympathetic tone P(LF) is also significantly associated with the SBPs variable (P(LF) has $B_{SBP} = 0.009$ with $P < 0.05$). The LLR test and F-statistics support the significant decrease in error variance and improvement in R^2. The change in error ranges from 6.38% to 13.2%.

Based on FDR ranking, we reported the asym(α) in QS and P(HF) in QS in **Figures 7 and 8** and we showed the results of simple main-effect analysis based on the ANOVA test. In a subset analysis of infants with <29 weeks GA, we found a significant SBP-by-measuring point interaction on rEEG asymmetry in quiet sleep (F(2,71) = 3.86, $P = 0.03$). Asymmetry decreased over time (main effect of measuring point: F(2,71) = 61.61, $P \leq 0.01$). At the

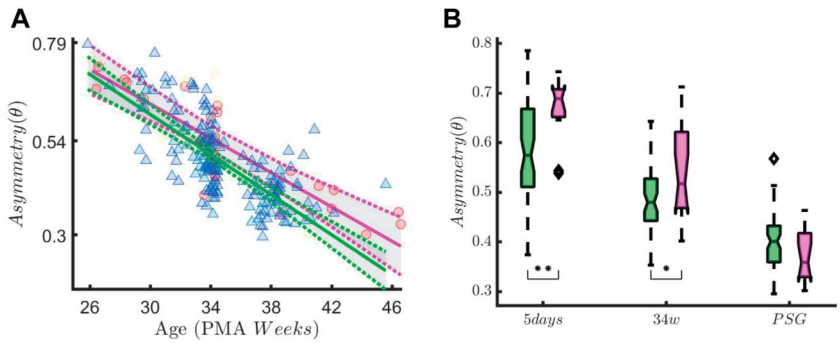

Figure 5. Range EEG asymmetry in QUIET sleep. The figure shows the association between rEEG asymmetry in the theta band (asymm) and early skin-breaking procedures (SBPs) Data are reported for the entire data set during QUIET sleep (QS). The left panel shows how the asymmetry maturational trend differs in case of high SBPs (magenta curve, SBPs ≥50) compared to low SBPs (green curve, SBP < 50). SBPs seem to increase the level of asymm throughout the development HF oscillations. The right panel shows the boxplot trend as output of the two-way ANOVA: the division between HIGH SBPs and LOW SBPs is reported for each recording time. The asymmetry decreases over time (main effect of measuring point: F(2,208) = 101.71, $P \leq 0.01$), but statistically significant interaction effect between measuring point and SBP group is found (F(2,208) = 8.52, $P \leq 0.01$). The simple main-effect analysis shows a higher asymmetry in the HIGH SBPs group at the 5-day recording ($P \leq 0.01$, indicated as ** in the figure) and a marginal significant difference for the 34 weeks ($P = 0.05$, indicated as * in the figure). The rEEG asymmetry does not statistically differ between HIGH and LOW SBPs groups at PSG recording time ($P = 0.72$). ANOVA, analysis of variance.

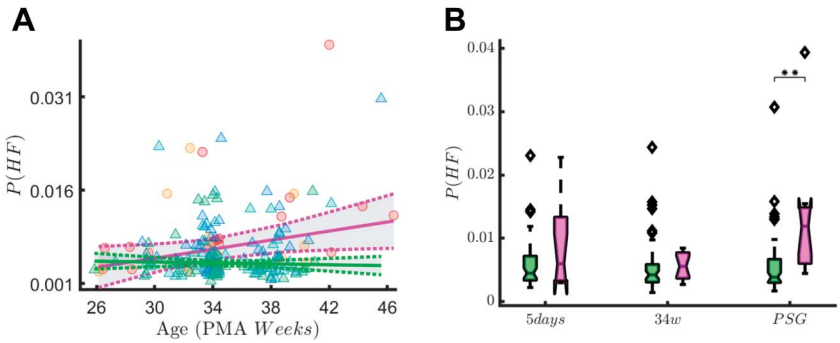

Figure 6. High-frequency oscillations in QUIET sleep. The figure shows the association between HF oscillations of the tachogram P(HF) and early skin-breaking procedure (SBPs). Data are reported for the entire data set during QUIET sleep (QS). The left panel show how P(HF) maturational trend differs in case of high SBPs (magenta curve, SBP ≥50) compared to low SBPs (green curve, SBP < 50). SBPs seem to increase the power of HF oscillations. The right panel shows the boxplot trend as output of the two-way ANOVA: the division between HIGH SBPs and LOW SBPs is reported for each recording time. The HF oscillations increases over time (main effect of measuring point: $F(2,191) = 5.97$, $P \leq 0.01$), but statistically significant interaction effect between measuring point and SBP group is found ($F(2,191) = 4.56$, $P \leq 0.01$). The simple main-effect analysis shows a higher P(HF) in HIGH SBPs group at the PSG recording time ($P \leq 0.01$, indicated as ** in the figure), but there is no difference for the 5-day ($P = 0.43$) or 34w ($P = 1$) recording time. ANOVA, analysis of variance; HF, high-frequency; SBP, skin-breaking procedures.

34-week recording, infants in the high SBP group showed a significantly higher rEEG asymmetry than the infants in the low SBP group ($P = 0.02$). At the recording at 5 days and the PSG recording, this difference did not reach significance ($P = 0.91$ and $P = 0.98$, respectively). A significant SBP-by-measuring point interaction on P(HF) is found in quiet sleep ($F(2,67) = 3.49$, $P = 0.04$). High-frequency oscillations also increase over time (main effect of measuring point: $F(2,67) = 6.49$, $P \leq 0.01$). Post hoc analysis showed that this difference in HF oscillations between the high and low SBP groups is only significantly different at the last, PSG, recording ($P = 0.04$).

4. Discussion

In this study, we confirmed our hypothesis that a high number of early skin-breaking procedures in premature infants are associated with a dysmature EEG. We also found that a high amount of SBPs is associated with a higher heart-rate variability.

Data were collected in a neonatal unit where a lot of attention is given to monitoring and minimizing pain and discomfort, and where individualized developmental care and family integrated care principles are fundamental to the unit's care philosophy. Nevertheless, this study confirms that preterm infants experience a high amount of skin-breaking procedures during their NICU stay.

Table 6

Results of the linear mixed-effect model for the quiet sleep (QS) state in the patients with a GA below 29 wks.

Feature	B_{SBP}	B_{GA}	B_{PMA}	MSE	R^2	R^2_{Red}	F_{LLR}	Δ(%)
P(HF)	0.005†	0.002†	0.00057*	0.00003	0.27	0.16	10.48†	13.2
Asym(α)	0.064‡	0.006§	−0.021*	0.005	0.7	0.58	6.52‡	8.43
P(LF)	0.009‡	0.002§	0.001*	0.00014	0.31	0.18	7.9‡	10.1
Asym(θ)	0.05‡	0.005§	−0.024*	0.005	0.74	0.66	4.88§	6.38

Only the features that have a significant association with early skin-breaking procedure are reported. The values B represent the fixed-effect coefficients for the SBP, GA, and PMA variables with the associated significance level (*P* value). For each feature, the following parameters are reported: the mean-absolute error (MSE), the coefficient of determination R^2, the coefficient of determination of the model with only GA and PMA (R^2_{Red}), the log-likelihood ratio (LLR) F-statistics, the decrease of error variance Δ(%) with SBP variable, and the two-way ANOVA *P* value associated to the SBP main effect. The *P* value is indicated with following symbols: * for *P* value ≤ 0.0001, † for $P \leq 0.01$, ‡ for $P \leq 0.05$, and § for not significant *P* values. P(HF) and P(LF) stand for HF and LF power in the tachogram, respectively, whereas asymmetry is the asymmetry of rEEG in the different frequency bands.

ANOVA, analysis of variance; GA, gestational age; NICU, neonatal intensive care unit; SBP, skin-breaking procedures; PMA, postmenstrual age.

Developmental studies show that both EEG and HRV are expected to change with infant's development. If electrophysiological patterns in these signals keep the traits and graphoelements, which are typical of early GA, they are labelled as dysmature. The 2 main features of dysmature EEG, which are discontinuity and slow-wave persistence, are all expected to significantly decrease with development (Pavlidis et al, 2017b; Wallois, 2010). As demonstrated in previous studies,[41,55] EEG complexity increases with increasing PMA, whereas range EEG asymmetry is higher in the first week of life and has a downward trend with development. For HRV, the band-power of the main HRV tones (VLF, LF, and HF) are all expected to increase with infants' development.[9,12,25]

To the best of our knowledge, this is the first study that shows the effect of pain-related stress on the functional maturation of the brain and the autonomic nervous system in premature infants. Our results show that a high number of early skin-breaking procedures is significantly associated to an EEG with lower EEG complexity and higher rEEG asymmetry, which can imply a dysmature EEG[31,32,41,55] and a higher HRV. Although the level of SBPs is strongly correlated with GA and PMA (**Tables 2 and 3**) as expected, the association between EEG and HRV variables and SBPs was not only confirmed after controlling for age at birth and age at recording, but was also supported by the decrease in prediction error when procedural pain was entered in the model. Simple main-effect analyses shows at which recording time the functional variables statistically differ between high and low SBPs groups. Post hoc analyses confirm that EEG shows dysmature traits in the first weeks of life, whereas the vagal tone is higher at PSG in the infants that experience a high amount of SBPs. Similar results were obtained in the early-GA group in terms of an association between high SBPs, dysmature EEG, and greater HRV. Interestingly, the results tend to be similar in the QS state (**Tables 5 and 6**), whereas no significant differences were found in nQS for the early-GA group compared to the entire data set.

Early pain might act on the infant's development through different mechanisms, mainly sensitization to pain of the central nervous system and lowering sensory threshold.[19] Early pain and injuries might developmentally regulate nociceptive pathways, such as hyperinnervation of the periphery and increasing receptive fields of the dorsal horn of neurons.[46,50] This peripheral

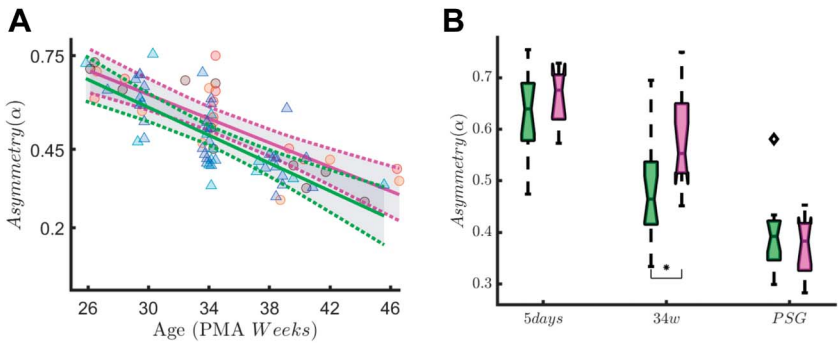

Figure 7. Range EEG asymmetry in early-GA patients. The figure shows the association between the rEEG asymmetry in the alpha band (asymm, Left Panel A) and early skin-breaking procedures (SBPs). Data are reported for the patients with gestational age below 29 weeks during QUIET sleep (QS). The left panel shows how the asymm trend differs in case of high SBPs (magenta curve, SBP ≥50) compared to low SBPs (green curve, SBP <50). Skin-breaking procedures seem to increase the level of asymm throughout the development. The right panel shows the boxplot trend as output of the two-way ANOVA: the division between HIGH SBPs and LOW SBPs is reported for each recording time. A significant SBP-by-measuring point interaction on rEEG asymmetry is found in quiet sleep ($F(2,71) = 3.86$, $P = 0.03$). Asymmetry also decreases over time (main effect of measuring point: $F(2,71) = 61.61$, $P \leq 0.01$). At the 34-week recording, infants in the high SBP group showed a significantly higher rEEG asymmetry than the infants in the low SBP group ($P = 0.02$, indicated as * in the figure). At the recording at 5 days and the PSG recording, this difference did not reach significance ($P = 0.91$ and $P = 0.98$, respectively). ANOVA, analysis of variance; GA, gestational age; rEEG, range EEG.

sensitization might lead to the central sensitization, which can affect the central nociceptive pathways and thalamus. Consequently, the thalamocortical projections will be abnormally distributed because their topography and structural organization are activity-dependent.[17] In premature infants, any impact on the thalamus development and thalamocortical connections will have a direct impact on the cortical activity because the high-amplitude delta bursts type of activity is a result of the predominance of the subcortical centers.[29,43] During the development of thalamocortical projections, the axons of the thalamus will contend the activity on the cortex. If early pain disrupts the thalamocortical connections, the activity on the cortex will also be different.[17]

Previous research showed that pain stimulation might induce higher delta activity and delta brushes, which are diffused over the entire cortex due to underdeveloped cortico-cortical connections, as also supported by fMRI studies.[52] This widespread diffused delta activity is present up to 35 weeks of GA, before it is replaced by a mature cortical response at full-term age.[47] We therefore speculated that neonatal pain might induce a different brain rhythmicity, especially in terms of δ band, and might lead to a greater discontinuous tracing on the cortex, as also shown in **Figures 4–6**. Because pain-related stress and cumulated pain might ultimately induce a diffused delta-burst activity,[18,26,47] pain can ultimately increase the discontinuity of the EEG and contribute to a more dysmature pattern. Therefore, the greater rEEG asymmetry and the lower EEG complexity are the result of a more dysmature tracing.

Clearly, other subtle factors or causes of this persistence EEG dysmaturity cannot be excluded. However, Doesburg et al[16] also found that a different brain rhythmicity was associated with cumulated pain, which was associated to reduced visual–perceptual abilities, and Grunau et al. showed that pain-related stress is associated with a lower cognitive outcome.[22] In parallel, several authors have shown that a dysmature EEG in premature infants is associated with worse cognitive outcome.[6,28,54] Furthermore, early-life pain and the resulting disruption of thalamocortical pathways are also associated with a lower cognitive outcome.[17] Therefore, our results might provide the functional link that can discriminate infants at risk for developmental delay: a higher SBP load might induce a more

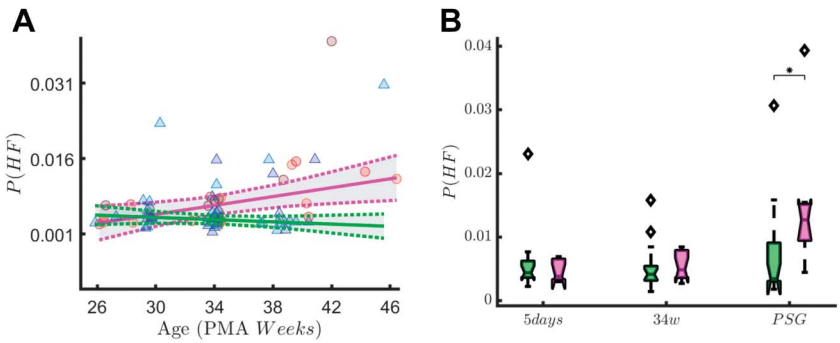

Figure 8. High-frequency oscillations in early-GA patients. The figure shows the association with the vagal tone (P(HF)) and early skin-breaking procedures (SBPs). Data are reported for the patients with gestational age below 29 weeks (n = 31) during QUIET sleep (QS). The left panel shows how the P(HF) maturational trend differs in case of high SBPs (magenta curve, SBP ≥50) compared to low SBPs (green curve, SBP <50). SBPs seem to increase the power of HF oscillations. The right panel shows the boxplot trend as output of the two-way ANOVA: the division between HIGH SBPs and LOW SBPs is reported for each recording time. The *P*-value associated to the ANOVA is reported on y-axis, whereas the output of the Tukey–Kramer multiple comparison test is reported below each boxplots group. A significant SBP-by-measuring point interaction on P(HF) is found in quiet sleep ($F(2,67) = 3.49$, $P = 0.04$). High-frequency oscillations also increases over time (main effect of measuring point: $F(2,67) = 6.49$, $P \leq 0.01$). Post hoc analysis showed this difference in HF oscillations between the HIGH and LOW SBP group is only significantly different at the last, PSG, recording ($P = 0.04$, indicated as * in the figure). ANOVA, analysis of variance; GA, gestational age; HF, high-frequency.

dysmature EEG, which is related to a lower development outcome. Currently, follow-up developmental testing is taking place in our patient sample so we will be able to link the current results with developmental outcome measures in the future.

Unlike EEG, the results related to HRV are somewhat counterintuitive. Normally, a lower heart-rate variability in premature infants is associated to a lower mental outcome[25] and the maturation of autonomic nervous system is characterized by an increase in short-term and long-term HRV, which means an increase in HF and LF oscillations.[12] Based on the cortical findings, one would expect that a higher SBP would decrease the HRV power in different bands. However, both HF and LF oscillations seem to increase with increasing age and increasing SBP. The increase in short-term and long-term variations of the tachogram might be the consequence of a faster autonomic nervous system development to modulate the noxious response. This might be a further consequence of central pain sensitization and the alteration of the stress response at autonomic nervous system control level and the HPA axis.[17,21,53] However, this hypothesis requires further testing in future studies.

A notable difference regards the sleep states: QS substantially presents more significant associations between stress and functional features than nQS. Similar to HRV, definitive conclusions cannot be drawn, but it is interesting to note that the greater number of associations are revealed in the calmest behavioral state with the most discontinuous EEG tracing.[1] This can be a further proof that early-life stress can induce a more discontinuous EEG, with a long-lasting effect to infant's physiology that goes beyond a simple sleep interruption or deprivation. However, QS is the latest state to mature and is typically characterized by a discontinuous tracing, which is one of the main traits of dysmaturity.[1] Therefore, the association between stress and dysmaturity might be easier to investigate in this stage than in nQS, which is normally a mix of active sleep and awake with a more continuous tracing.

Another crucial point regards the most vulnerable patients, who have GA ≤29 weeks. Duerden et al. found a stronger association between SBPs and the thalamic volume[17] in extremely preterm infants. One might expect that the association between SBPs and EEG dysmaturity is mainly driven by the young GA of the patients with high SBPs. We did, however, confirm the link between high SBPs, EEG dysmaturity, and higher HRV in the GA ≤29 weeks subgroup. Therefore, the current results show similar EEG dysmaturity and HRV behavior for both the entire data set and the vulnerable patient group in case of high SBPs. Interestingly, this similarity is present only for the QS state, whereas the results were not confirmed during nQS in the early-GA group. This similarity in the calmest state of the sleep cycle might further support the long-lasting effect of stress on sleep architecture and physiology.

5. Conclusions

The current study aimed to quantify the association between early SBPs and EEG and HRV functional trends in preterm infants. We found a more discontinuous EEG and a larger HRV in infants that were exposed to high levels of early procedural pain. These dysmaturity patterns provide further evidence that central pain sensitization in premature babies might affect their future development and cognitive and behavioural outcome. Pain and stress assessment through functional monitoring might help clinicians to optimize their pain treatment at cot-side. Because the early-life experience in the first days of life is crucial for future development, the use of EEG and HRV might complement clinicians' guideline about analgesia to ameliorate the neurodevelopmental outcome of the patients.

Conflict of interest statement

The authors have no conflicts of interest to declare.

Acknowledgements

The authors thank all children and parents who participated in the study. They are also thankful to the research nurses Isabelle Hermans and Julie Messiaen, and student Elien De Saeger for the support in the SBP collection and to technicians Katrien Lemmens and Jan Vervisch for the EEG measurements. Research supported by Bijzonder Onderzoeksfonds KU Leuven (BOF): C24/15/036 "The effect of perinatal stress on the later outcome in preterm babies," EU: H2020 MSCA-ITN-2018: "INtegrating Functional Assessment measures for Neonatal Safeguard (INFANS)," funded by the European Commission under Grant Agreement #813483. This research received funding from the Flemish Government (AI Research Program). SVH and ML are affiliated to Leuven.AI—KU Leuven institute for AI, B-3000, Leuven, Belgium. Mario Lavanga is a SB PhD. fellow at Fonds voor Wetenschappelijk Onderzoek (FWO), Vlaanderen, supported by the Flemish government.

Article history:
Received 16 May 2020
Received in revised form 19 October 2020
Accepted 21 October 2020
Available online 26 October 2020

References

[1] André M, Lamblin MD, d'Allest AM, Curzi-Dascalova L, Moussalli-Salefranque F, Nguyen The Tich S, Vecchierini-Blineau MF, Wallois F, Walls-Esquivel E, Plouin P. Électroencéphalographie du nouveau-né prématuré et à terme. Aspects maturatifs et glossaire. Neurophysiol Clin 2010;40:59–124.
[2] Ansari AH, De Wel O, Lavanga M, Caicedo A, Dereymaeker A, Jansen K, Vervisch J, De Vos M, Naulaers G, Van Huffel S. Quiet sleep detection in preterm infants using deep convolutional neural networks. J Neural Eng 2018;15:066006.
[3] Bailón R, Laouini G, Grao C, Orini M, Laguna P, Meste O. The integral pulse frequency modulation model with time-varying threshold: application to heart rate variability analysis during exercise stress testing. IEEE Trans Biomed Eng 2011;58:642–52.
[4] Barrett AB, Barnett L, Seth AK. Multivariate Granger causality and generalized variance. Phys Rev E 2010;81:041907.
[5] Bhutta AT, Cleves MA, Casey PH, Cradock MM, Anand KJSS, Children S, Cleves MA, Casey PH, Cradock MM, Anand KJSS. Cognitive and behavioral outcomes of school-aged children who were born preterm. J Am Med Assoc 2007;288:728–37.
[6] Le Bihannic A, Beauvais K, Busnel A, de Barace C, Furby A. Prognostic value of EEG in very premature newborns. Arch Dis Child Fetal Neonatal 2012;97:F106–9.
[7] Bosl W, Tierney A, Tager-Flusberg H, Nelson C. EEG complexity as a biomarker for autism spectrum disorder risk. BMC Med 2011;9:18.
[8] Brummelte S, Grunau RE, Chau V, Poskitt KJ, Brant R, Vinall J, Gover A, Synnes AR, Miller SP. Procedural pain and brain development in premature newborns. Ann Neurol 2012;71:385–96.
[9] Clairambault J, Curzi-dascalovab L, Kauffmann F, Mkdiguea C. Heart rate variability in normal sleeping and preterm neonates full-term. Early Hum Dev 1992;28:169–83.
[10] Cong X, Ludington-Hoe SM, McCain G, Fu P. Kangaroo Care modifies preterm infant heart rate variability in response to heel stick pain: pilot study. Early Hum Dev 2009;85:561–7.
[11] Costa M, Goldberger AL, Peng CKK. Multiscale entropy analysis of complex physiologic time series. Phys Rev Lett 2002;89:068102-1 - 068102-4.

[12] Curzi-Dascalova L. Development of sleep and autonomic nervous system contorl in premature and full-term newborns. Arch Pediatr 1994;2: 255–62.
[13] David M, Hirsch M, Karin J, Toledo E, Akselrod S. An estimate of fetal autonomic state by time-frequency analysis of fetal heart rate variability. J Appl Physiol 2007;102:1057–64.
[14] Dereymaeker A, Pillay K, Vervisch J, Van Huffel S, Naulaers G, Jansen K, De Vos M. An automated quiet sleep detection approach in preterm infants as a gateway to assess brain maturation. Int J Neural Syst 2017: 1750023.
[15] Dick OE. Multifractal analysis of the psychorelaxation efficiency for the healthy and pathological human brain. Chaotic Model Simul 2012;1: 219–27.
[16] Doesburg SM, Chau CM, Cheung TPL, Moiseev A, Ribary U, Herdman AT, Miller SP, Cepeda IL, Synnes A, Grunau RE. Neonatal pain-related stress, functional cortical activity and visual-perceptual abilities in school-age children born at extremely low gestational age. PAIN 2013;154: 1946–52.
[17] Duerden EG, Grunau RE, Guo T, Foong J, Pearson A, Au-Young S, Lavoie R, Chakravarty MM, Chau V, Synnes A, Miller SP. Early procedural pain is associated with regionally-specific alterations in thalamic development in preterm neonates. J Neurosci 2018;38:878–86.
[18] Fabrizi L, Slater R, Worley A, Meek J, Boyd S, Olhede S, Fitzgerald M. A shift in sensory processing that enables the developing human brain to discriminate touch from pain. Curr Biol 2011;21:1552–8.
[19] Fitzgerald M. The development of nociceptive circuits. Nat Rev Neurosci 2005;6:507–20.
[20] Ghosh D, Chen W, Raghunathan T. The false discovery rate: a variable selection perspective. J Stat Plan Inference 2006;136:2668–84.
[21] Grunau RE. Neonatal pain in very preterm infants: long-term effects on brain, neurodevelopment and pain reactivity. Rambam Maimonides Med J 2013;4:e0025.
[22] Grunau RE, Whitfield MF, Petrie-Thomas J, Synnes AR, Cepeda IL, Keidar A, Rogers M, Mackay M, Hubber-Richard P, Johannesen D. Neonatal pain, parenting stress and interaction, in relation to cognitive and motor development at 8 and 18 months in preterm infants. PAIN 2009;143:138–46.
[23] Hoyer D, Tetschke F, Jaekel S, Nowack S, Witte OW, Schleußner E, Schneider U. Fetal functional brain age assessed from universal developmental indices obtained from neuro-vegetative activity patterns. PLoS One 2013;8:1–8.
[24] Isler JR, Stark RI, Grieve PG, Welch MG, Myers MM. Integrated information in the EEG of preterm infants increases with family nurture intervention, age, and conscious state. PLoS One 2018;13:e0206237.
[25] Javorka K, Lehotska Z, Kozar M, Uhrikova Z, Kolarovszki B, Javorka M, Zibolen M. Heart rate variability in newborns. Physiol Res 2017;66: 203–14.
[26] Jones L, Fabrizi L, Laudiano-Dray M, Whitehead K, Meek J, Verriotis M, Fitzgerald M. Nociceptive cortical activity is dissociated from nociceptive behavior in newborn human infants under stress. Curr Biol 2017;27: 3846–51.e3.
[27] Kim SB, Chen VCP, Park Y, Ziegler TR, Jones DP. Controlling the false discovery rate for feature selection in high-resolution NMR spectra. Stat Anal Data Min 2008;1:57–66.
[28] Kong AHT, Lai MM, Finnigan S, Ware RS, Boyd RN, Colditz PB. Background EEG features and prediction of cognitive outcomes in very preterm infants: a systematic review. Early Hum Dev 2018;127:74–84.
[29] Kostovic I, Judas M. The development of the subplate and thalamocortical connections in the human foetal brain. Acta Paediatr Int J Paediatr 2010;99:1119–27.
[30] Lake DE, Richman JS, Griffin MP, Moorman JR. Sample entropy analysis of neonatal heart rate variability. Am J Physiol Integr Comp Physiol 2002; 283:R789–97.
[31] Lavanga M, De Wel O, Caicedo A, Heremans E, Jansen K, Dereymaeker A, Naulaers G, Van Huffel S. Automatic quiet sleep detection based on multifractality in preterm neonates: effects of maturation. Proceedings of the 39th Annual International Conference of the IEEE Engineering in Medicine and Biology Society (EMBC). IEEE, 2017. pp. 2010–2013. doi: 10.1109/EMBC.2017.8037246.
[32] Lavanga M, De Wel O, Caicedo A, Jansen K, Dereymaeker A, Naulaers G, Van Huffel S. A brain-age model for preterm infants based on functional connectivity. Physiol Meas 2018;39:044006.
[33] Linsell L, Johnson S, Wolke D, Morris J, Kurinczuk JJ, Marlow N. Trajectories of behavior, attention, social and emotional problems from childhood to early adulthood following extremely preterm birth: a prospective cohort study. Eur Child Adolesc Psychiatry 2019;28:531–42.
[34] Linsell L, Johnson S, Wolke D, O'Reilly H, Morris JK, Kurinczuk JJ, Marlow N. Cognitive trajectories from infancy to early adulthood following birth before 26 weeks of gestation: a prospective, population-based cohort study. Arch Dis Child 2018;103:363–70.
[35] Marret S, Ancel PY, Marpeau L, Marchand L, Pierrat V, Larroque B, Foix-L'Hélias L, Thiriez G, Fresson J, Alberge C, Rozé JC, Matis J, Bréart G, Kaminski M. Neonatal and 5-year outcomes after birth at 30-34 weeks of gestation. Obstet Gynecol 2007;110:72–80.
[36] Mento G, Bisiacchi PS. Neurocognitive development in preterm infants: insights from different approaches. Neurosci Biobehav Rev 2012;36: 536–55.
[37] Moeyersons J, Amoni M, Huffel SVan, Willems R, Varon C; R-DECO. An open-source Matlab based graphical user interface for the detection and correction of R-peaks. bioRxiv 2019:560706.
[38] O'Toole JM, Boylan GB. NEURAL: quantitative features for newborn EEG using Matlab. arXiv Prepr arXiv170405694. 2017. Available at: http://arxiv.org/abs/1704.05694. Accessed November 27, 2019.
[39] O'Toole JM, Boylan GB. Quantitative preterm EEG analysis: the need for caution in using modern data science techniques. Front Pediatr 2019;7: 174.
[40] O'Toole JM, Boylan GB, Vanhatalo S, Stevenson NJ. Estimating functional brain maturity in very and extremely preterm neonates using automated analysis of the electroencephalogram. Clin Neurophysiol 2016;127:2910–18.
[41] O'Toole JM, Pavlidis E, Korotchikova I, Boylan GB, Stevenson NJ. Temporal evolution of quantitative EEG within 3 days of birth in early preterm infants. Sci Rep 2019;9:1–12.
[42] Pavlidis E, Lloyd RO, Boylan GB. EEG-A valuable biomarker of brain injury in preterm infants. Dev Neurosci 2017;39:23–35.
[43] Pavlidis E, Lloyd RO, Mathieson S, Boylan GB. A review of important electroencephalogram features for the assessment of brain maturation in premature infants. Acta Paediatr Int J Paediatr 2017; 106:1394–408.
[44] Popivanov D, Stomonyakov V, Minchev Z, Jivkova S, Dojnov P, Jivkov S, Christova E, Kosev S. Multifractality of decomposed EEG during imaginary and real visual-motor tracking. Biol Cybern 2006;94:149–56.
[45] Ranger M, Chau CMY, Garg A, Woodward TS, Beg MF, Bjornson B, Poskitt K, Fitzpatrick K, Synnes AR, Miller SP, Grunau RE. Neonatal pain-related stress predicts cortical thickness at age 7 Years in children born very preterm. PLoS One 2013;8:e76702.
[46] Reynolds ML, Fitzgerald M. Long-term sensory hyperinnervation following neonatal skin wounds. J Comp Neurol 1995;358:487–98.
[47] Slater R, Fabrizi L, Worley A, Meek J, Boyd S, Fitzgerald M. Premature infants display increased noxious-evoked neuronal activity in the brain compared to healthy age-matched term-born infants. Neuroimage 2010; 52:583–9.
[48] Smith GC, Gutovich J, Smyser C, Pineda R, Newnham C, Tjoeng TH, Vavasseur C, Wallendorf M, Neil J, Inder T. Neonatal intensive care unit stress is associated with brain development in preterm infants. Ann Neurol 2011;70:541–9.
[49] The International Neonatal Network. The CRIB (clinical risk index for babies) score: a tool for assessing initial neonatal risk and comparing performance of neonatal intensive care units. Lancet 1993;342: 193–8.
[50] Torsney C, Fitzgerald M. Spinal dorsal horn cell receptive field size is increased in adult rats following neonatal hindpaw skin injury. J Physiol 2003;550:255–61.
[51] Valenza G, Citi L, Lanata A, Gentili C, Barbieri R, Scilingo EP. Applications of heartbeat complexity analysis to depression and bipolar disorder. In: Complexity and Nonlinearity in Cardiovascular Signals. Cham: Springer International Publishing, 2017. p. 345–74. doi:10.1007/978-3-319-58709-7_13.
[52] Verriotis M, Chang P, Fitzgerald M, Fabrizi L. The development of the nociceptive brain. Neuroscience 2016;338:207–19.
[53] Vinall J, Grunau RE. Impact of repeated procedural pain-related stress in infants born very preterm. Pediatr Res 2014;75:584–7.
[54] Watanabe K, Hayakawa F, Okumura A. Neonatal EEG: a powerful tool in the assessment of brain damage in preterm infants. Brain Dev 1999;21: 361–72.
[55] De Wel O, Lavanga M, Dorado A, Jansen K, Dereymaeker A, Naulaers G, Van Huffel S. Complexity analysis of neonatal EEG using multiscale entropy: applications in brain maturation and sleep stage classification. Entropy 2017;19:516.
[56] Zhang D, Ding HH, Liu Y, Zhou C, Ding HH, Ye D. Neurodevelopment in newborns: a sample entropy analysis of electroencephalogram. Physiol Meas 2009;30:491–504.